Power, Energy and Electrical Engineering
M. Deng (Ed.)

doi:10.3233/ATDE240314

Enhancing Wind Turbine Efficiency Within the Eolic Cell: A Metamodel-Driven Approach

Giusep Baca [a,1], Alfredo R. Calle [a] and Salome Gonzales [a]
[a] *Faculty of Mechanical Electrical Engineering, National University of Engineer, Lima, Peru*

Abstract. In the pursuit of sustainable energy solutions, wind power emerges as a pivotal contender. This research pioneers the integration of a Horizontal Axis Wind Turbine (HAWT) into the Eolic Cell—a modular wind energy system designed for augmented wind speed and efficiency. Our primary objective is the holistic optimization of HAWT performance, considering five distinct Tip Speed Ratios (TSR) to account for varying conditions. To optimize turbine performance, we manipulate three key parameters: pitch angles of turbine blades along the radius, the First-Grade coefficient, the Second-Grade coefficient, and the NACA profile chord. A novel Metamodel of Optimal Prognosis (MOP) methodology is introduced, streamlining computational efficiency and facilitating gradient-based optimization across the chosen TSRs. This research marks a significant stride in advancing wind energy solutions for distributed generation, focusing on practical efficiency enhancements. It leverages innovative approaches in wind power generation, laying the groundwork for a sustainable energy future. This article signifies the initial phase of our exploration into harnessing the potential of Eolic Cells as a transformative solution for distributed energy generation, with future research endeavors aimed at validating its practicality.

Keywords. Horizontal Axis Wind Turbine (HAWT), Eolic Cell, Tip Speed Ratios (TSR), Metamodel of Optimal Prognosis (MOP)

1. Introduction

The pursuit of renewable energy solutions is gaining momentum as the world races to achieve Net Zero Emission (NZE) targets by 2050 [1]. This endeavor is critical, given that nearly half of the necessary emissions reductions rely on technologies still in prototype or demonstration phases [1]. Renewable capacity is on the rise, but the trajectory and government commitments may not align with NZE goals, presenting challenges in financing, permitting, societal acceptance, grid integration, and supply chain dynamics [2]. To bridge this gap, innovative wind power generation approaches are essential.

This research explores the integration of a Horizontal Axis Wind Turbine (HAWT) into the Eolic Cell—a modular wind energy system designed for enhanced wind speed and efficiency. The primary focus is a comprehensive optimization of HAWT performance, encompassing three pivotal parameters: pitch angles of turbine blades along the radius, the First-Grade coefficient, the Second-Grade coefficient, and the NACA profile chord. Unlike conventional single-parameter optimization, our approach is holistic, optimizing turbine performance across a spectrum of conditions, including

[1] Corresponding Author, Giusep Baca, Faculty of Mechanical Electrical Engineering, National University of Engineer, Lima, Peru; E-mail: gbacab@uni.pe.

five distinct Tip Speed Ratios (TSR), thereby introducing multidimensionality into the research.

Building on pioneering work in wind energy, we address the pressing need for efficiency enhancements in distributed energy generation. We introduce a Metamodel of Optimal Prognosis (MOP) as a methodological innovation [3-5], allowing for efficient optimization across the various TSRs. This approach streamlines computational expenses while identifying an ideal turbine profile within the performance envelope defined by these TSRs, a crucial step toward efficient turbine optimization.

This article signifies the initial chapter in an ongoing exploration of Eolic Cells' potential for revolutionizing distributed energy generation. Future endeavors will encompass exhaustive experimentation, validating the viability of this groundbreaking approach. Furthermore, it is worth noting that this study builds upon and extends previous research focused on optimizing the Eolic Cell itself [6]. This new phase incorporates a turbine and extends the scope of optimization, synergizing both components for enhanced wind energy generation.

2. Heading

The Eolic Cell, a foundational component of the innovative wind energy system, is explored in this chapter. This versatile unit plays a pivotal role in augmenting wind velocity and, subsequently, enhancing the efficiency of wind energy generation. While the Eolic Cell is a building block of the larger Eolic Wall structure, our focus here remains on its individual attributes.

An Eolic Cell is an aerodynamic structure designed to boost wind velocity, composed of two main sections: the Adjacent External Section (AES) and the Internal Aerodynamic Chamber (IAC). The AES serves as an external adjoining wall shared between adjacent Eolic Cells, allowing for their seamless arrangement. The IAC, the heart of the Eolic Cell, is where wind velocity undergoes a carefully orchestrated transformation (Figure 1).

The IAC, further divided into three sections, holds unique characteristics. The anterior section, exposed to incoming wind, experiences high drag force and pressure levels, featuring an inlet opening for wind entry. Positioned between the anterior and posterior sections, the throat section witnesses the lowest pressure levels and the highest wind velocities, making it a critical region for wind energy augmentation.

The posterior section guides airflow towards an outlet opening while minimizing turbulence within the IAC.

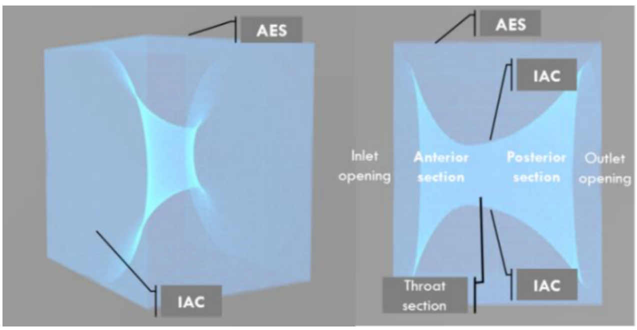

Figure 1. Eolic Cell’s sections [6].

Computational Fluid Dynamics (CFD) simulations provide valuable insights into the pressure and wind velocity fields around the Eolic Cell. They emphasize the importance of the IAC's shape in optimizing wind velocity, with streamlined shapes proving significantly more efficient.

This chapter underscores the significance of the Eolic Cell's unique design and aerodynamics in enhancing wind velocity. As we progress in this study, the integration of Horizontal Axis Wind Turbines (HAWT) within the Eolic Cell promises to unlock even greater advancements in harnessing renewable wind energy and fine-tuning its performance (Figure 2). Notably, these turbines find their optimal location within the throat section of the Eolic Cell, further enhancing their energy capture potential.

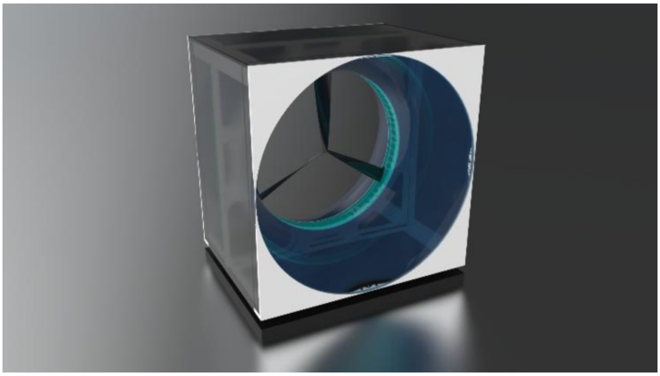

Figure 2. Horizontal axis wind turbine within the Eolic Cell.

3. CFD Methodology

3.1. Governing Equations and Turbulence Models

The simulation strategy involves a steady-state simulation within a 3D geometry, incorporating distinct domains for the stationary and rotating components. The reference frame method will enable the modeling of turbine rotation. The governing equations for incompressible and steady-state flow, namely continuity and momentum equations, will be utilized [7-8]. Finally, the K-ω SST turbulence model will be applied to accurately describe turbulent flow behavior within the Eolic cell and around the HAWT turbine [9-10].

3.2. Fluid Domain

The fluid domain for optimizing the Eolic Wall operates under specific conditions. These conditions involve an inlet velocity set at 8 m/s and a range of Tip Speed Ratios (TSR) encompassing 1.38, 1.55, 1.725, 1.8975, and 2.07. These particular TSR values were selected based on their previously observed high power coefficient (Cp) in simulations of the model.

Furthermore, the dimensions of the fluid domain adhere to established guidelines and are scaled according to the Eolic Cell turbine's diameter (Figure 3). It's worth noting that these guidelines were originally designed for 2D simulations. Therefore, both the height and width of the domain are set to the same value, maintaining consistency with the 2D modeling approach. This approach ensures that the domain dimensions align with the requirements and parameters necessary for the optimization process.

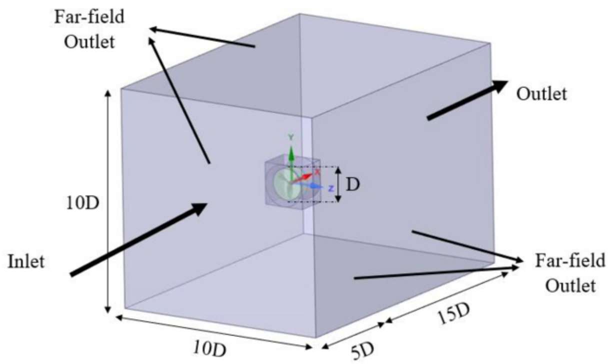

Figure 3. Computational domain dimensions of the Eolic Cell in function of its diameter.

3.3. Computational Mesh

The decision to utilize an unstructured mesh for the 3D Eolic wall turbine stems from its adaptability to complex geometries, a critical requirement for accurately representing the intricate details of both the Eolic Cell and the turbine within the computational domain. This meshing approach allows for precise boundary layer resolution, with a 25-boundary layer ensuring a y+ value of around 10 for the Eolic Cell and 1 for the turbine blades. This meticulous meshing enhances simulation accuracy, enabling a thorough analysis of the Eolic Wall's performance and optimization. The meshing specifics are shown in Table 1.

Table 1. Eolic Cell Meshing Metrics.

Metric	Orthogonal Quality	Skewness
Minimum	0.1534	0.0345
Maximum	0.9845	0.9745
Average	0.9354	0.0127
Standard deviation	0.1125	0.0324

3.4. Grid Convergence Analysis

In the Grid Convergence Analysis, we evaluated the Eolic cell domain using three different mesh types: refined, medium, and coarse. Utilizing the Grid Convergence Index (GCI) method as proposed by Celik [11], we assessed discretization errors. After conducting simulations and calculating average power coefficient values for each mesh, we found that the medium mesh displayed a negligible error of only 0.532%. This makes it a highly suitable choice for conducting CFD simulations with minimal uncertainty.

3.5. Validation Study and Parameter Calibration

To ensure the accuracy of our numerical simulations, we calibrated the Ansys Fluent 2022-R2 software using experimental data from a scaled prototype. The focus of this calibration was on turbulence parameters at the inlet boundary conditions. We transitioned from the "Intensity and Viscosity Ratio" to the "K and Omega" turbulence specification method and made specific adjustments to the default K and Omega parameters, as shown in the table below:

Table 2. Modifications for Turbulence Parameters.

Parameter	Default Value	Modified Value
Turbulent Kinetic Energy (K)	1.0	0.1910
Specific Dissipation Rate (Omega)	1.0	0.5455

These modifications were informed by a rigorous sensitivity analysis conducted using the OptiSlang software within Ansys Workbench. This calibration process involved 100 simulations, ensuring that our computational fluid dynamics (CFD) simulations accurately represent real-world conditions [6].

4. Response Surface Method

In this chapter, we delve into the Metamodel of Optimal Prognosis (MOP) [12]. The comprehensive methodology, which encompasses the CFD approach, response surface method, and optimization procedure, is encapsulated in Figure 4 for an overview.

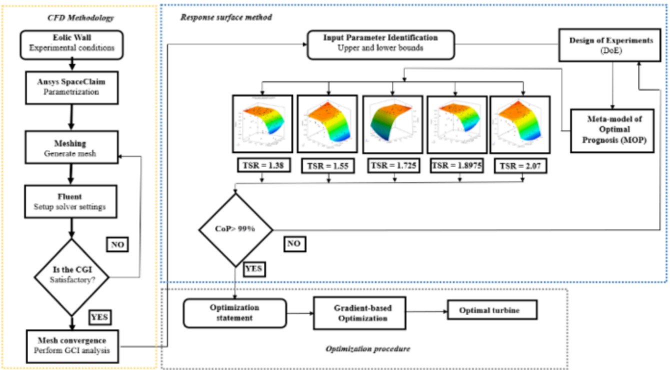

Figure 4. Computational domain dimensions of the Eolic Cell in function of its diameter.

4.1. Input Parameter Identification

As previously mentioned, our optimization process focuses on three key input parameters:

- NACA Profile Chord Length (C)

- Pitch Angle Along the Radius of the Turbine (controlled by two parameters)

To simplify the control of the pitch angle (β) along the radius (r) and reduce complexity, we utilize a second-order equation. The input parameters for this equation consist of the first-grade coefficient (FGC) and the second-grade coefficient (SGC), with a constant value of 0.

$$r * FGC + r^2 * SGC = \beta \tag{1}$$

4.2. Coefficient of Prognosis

The Coefficient of Performance (CoP) [13] is a key metric for evaluating the generalization capability of regression models with unknown data. It measures the fraction of explained variation in response predictions and is applicable to various types of response surfaces such as polynomial regressions, Moving Least Squares and Kriging.

- In practice, CoP can be visualized using data from analytical functions. Notable points include:

- CoP tends to increase with more samples, making it a conservative estimate.

- It should generally rise with an increasing number of samples, up to a certain limit.

- For continuous functions, CoP ideally converges to 1.

- In CAE models, it often converges to a value below 1 due to numerical noise.

Thus, understanding CoP helps assess the reliability of response surface models, aiding optimization efforts.

4.3. Single Variable Sensitivity

The Metamodel of Optimal Prognosis (MOP) allows us to assess the impact of individual parameters using variance-based sensitivity indices. These indices measure the fraction of variance explained by a single input variable.

The importance of each parameter is scaled with respect to the global Coefficient of Performance (CoP). In some cases, sensitivity indices may also account for coupling terms

It's essential to note that the sum of individual CoPs, when greater than the total CoP, indicates the presence of coupling terms, highlighting the interactions between input variables. This analysis provides valuable insights into the influence of individual parameters within the optimization framework.

4.4. Lower Bound and Upper Bound of the variables

The Computational Fluid Dynamics (CFD) inputs are determined by three primary parameters: NACA Profile Chord Length (C), first-grade coefficient (FGC), and the second-grade coefficient (SGC). To establish the range of these variables, considering the characteristics of the NACA airfoil, conservative lower and upper boundaries have been selected, as detailed in Table 3:

Table 3. Lower Bound and Upper Bound for The Variables.

Input variable	Lower bound (m)	Upper bound
C	0.075	0.125
FGC	7.5	12.5
SGC	-0.5875	-0.3525

For each Tip Speed Ratio (TSR), a comprehensive set of 100 simulations is conducted, resulting in a total of 500 simulations. This approach allows for a thorough exploration of the optimization space across different TSR values, ensuring a robust analysis of the Metamodel of Optimal Prognosis (MOP).

5. Optimization Procedure

5.1. Optimization Statement

This study aims to identify the optimal profile within a specified operational range, focusing on performance enhancement. The optimization process involves numerically integrating the $\overline{C_p} - TSR$ curve using the predetermined TSR values. For this purpose, gradient-based optimization methods were employed, ensuring unrestricted exploration within the defined boundaries. The optimization statement is as follows:

$$\text{Find } X = \{C, SGC, FGC\}^T \text{that} \qquad \text{maximizes the } \int_{TSR_0}^{TSR_f} \overline{C_p}.$$

5.2. Gradient Based Optimization

Gradient-based optimization offers a powerful approach for optimizing complex systems. Newton's method is a derivative-based technique ideal for uncertain solutions in Computer-Aided Engineering (CAE). Nonlinear Programming by Quadratic Langrangian (NLPQL) suits simpler problems with fewer design variables. For more complex tasks, the Downhill Simplex (Simplex) method, an iterative approach adjusting based on target function values, proves effective [14-15].

6. Results

6.1. Meta-model of Optimal Prognosis Assessment

After conducting CFD simulations using Ansys Fluent for LHS-based design point sampling, meta-models were developed for different TSRs, including Linear Regression

Models, Moving Least Squares, and Kriging. Among these, Kriging was identified as the most suitable method based on the CoP.
A 3D heatmap plotting the NACA chord (X-axis) length and FGC (Y-axis), with the Integral of the Cp-TSR curve on the Z-axis, is presented in Figure 5. Similarly, Figure 6 displays a 3D heatmap depicting the NACA chord (X-axis) length and SGC (Y-axis), with the Integral of the Cp-TSR curve on the Z-axis.

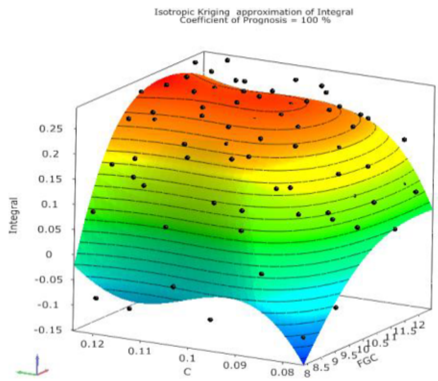

Figure 5. 3D heatmap plotting the NACA chord (X-axis) length and FGC (Y-axis), with the Integral of the Cp-TSR curve on the Z-axis.

The individual contribution of each input variable to the Integral of the Cp-TSR curve can be observed in Figure 7. This provides a clear insight into how each variable independently influences the final outcome. Additionally, Figure 7 demonstrates how changes in each of these input variables impact the value of the Integral of the Cp-TSR curve. As it shown Figure 7, the FGC has the highest contribution (58% main effect) over the output.

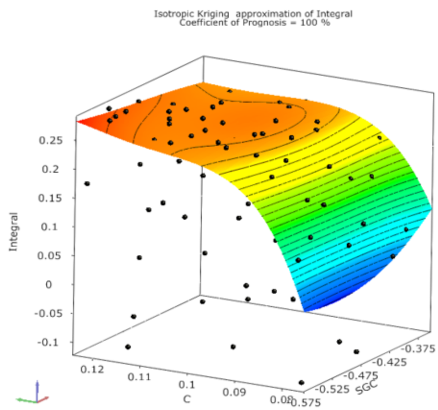

Figure 6. 3D heatmap plotting the NACA chord (X-axis) length and SGC (Y-axis), with the Integral of the Cp-TSR curve on the Z-axis.

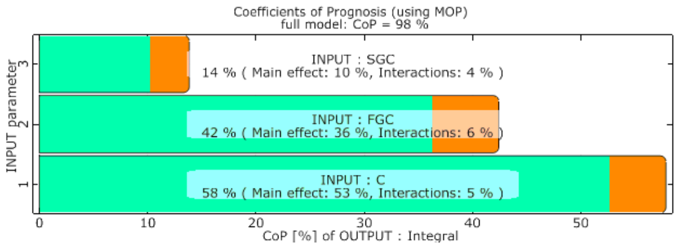

Figure 7. Individual contribution of each input variable

6.2. Optimization Results

Optimizations were carried out using two gradient-based methods: NLPQL and Simplex. With the NLPQL method, approximately 70 iterations were required to identify the maximum, as illustrated in Figure 8.

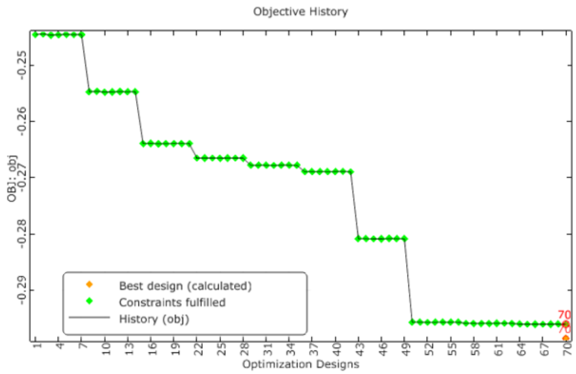

Figure 8. Number of iterations performed by NLPQL to reach the optimization objective maximum.

Similarly, the Simplex method also required about 70 iterations to reach the maximum, as shown in Figure 9.

The following table presents the combination of points resulting in the optimal turbine design for each methodology:

Table 4. Results of Simulations of the Optimal Points.

	C	FGC	SGC	Prediction	Simulation	Error
NLPQL	0.1243	11.22	0.5775	0.2960	0.29861	0.8817%
Simplex	0.1240	11.31	0.5761	0.2948	0.29843	1.2313%

As seen in Table 4, the differences between both optimization methods are minimal. However, the NLPQL method proposes a parameter combination that yields a more accurate prediction and a lower error when corroborated with the simulation results.

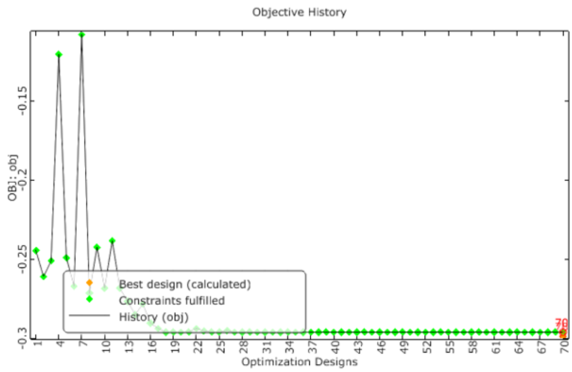

Figure 9. Number of iterations performed by Simplex to reach the optimization objective maximum

6.3. Optimal Profile

Based on the above, a simulation of the optimal point for the NLPQL model was executed, covering a broader range of rotation speeds. The aim was to observe the behavior of the Cp-TSR curve.

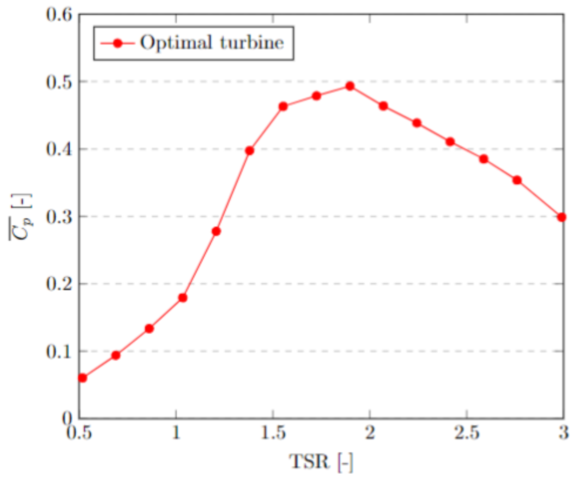

Figure 10. Performance of the new optimal turbine**.**

The figure 10 illustrates the performance of the optimized turbine, highlighting a prediction of a maximum Cp of 0.49 at an incoming wind speed of 8 m/s.

7. Conclusions

- Kriging was found to be the most suitable method for meta-modeling, based on the CoP assessment.
- The First-Grade Coefficient (FGC) had the highest impact on the Integral of the Cp-TSR curve, contributing 58% to the main effect.

- Optimization using the NLPQL and Simplex methods required approximately 70 iterations to reach the maximum.

- The NLPQL method provided a more accurate prediction and lower error compared to simulations.

- Simulation of the optimal NLPQL model across a wider range of rotation speeds revealed a maximum Cp of 0.49 at an incoming wind speed of 8 m/s.

8. Future Works

In building upon the findings of this study, several avenues for future research are suggested. These include extending the metamodel-driven approach to a wider range of wind turbines and renewable energy systems to assess its broader applicability and efficiency. An in-depth investigation into the long-term durability and maintenance needs of the optimized turbine designs under varied environmental conditions is also recommended. Additionally, conducting economic analyses to explore the feasibility and cost implications of large-scale deployment of the Eolic Cell technology will be crucial. Further studies should also delve into the environmental impact and sustainability aspects of the Eolic Cell, particularly its role in carbon emissions reduction. The potential integration of this technology with smart grid systems presents an interesting area of research, focusing on the enhancement of energy distribution efficiency. Lastly, examining the influence of public policy and regulatory frameworks on the adoption and scaling of the Eolic Cell technology will provide valuable insights into its practical implementation and growth within the renewable energy sector.

Acknowledgment

This work was carried out with the financial support of PROCIENCIA for the project development, as per contract PE501078852.

References

[1] IEA, “World Energy Outlook 2021 – Analysis,” IEA, 2021. https://www.iea.org/reports/world-energy-outlook-2021
[2] IEA, “Renewables 2021 – Analysis,” IEA, 2021. https://www.iea.org/reports/renewables-2021
[3] T. W. Simpson, A. J. Booker, D. Ghosh, A. A. Giunta, P. N. Koch, and R.-J. . Yang, “Approximation methods in multidisciplinary analysis and optimization: a panel discussion,” *Structural and Multidisciplinary Optimization*, vol. 27, no. 5, Jun. 2004, doi: https://doi.org/10.1007/s00158-004-0389-9.
[4] D. C. Montgomery and G. C. Runger, *Applied statistics and probability for engineers*. Hoboken, Nj Wiley, 2018.
[5] A. Labijak-Kowalska and Miłosz Kadziński, “Exact and stochastic methods for robustness analysis in the context of Imprecise Data Envelopment Analysis,” *Operational Research*, vol. 23, no. 1, Mar. 2023, doi: https://doi.org/10.1007/s12351-023-00755-z.
[6] Calle, Alfredo R., et al. “Optimization of the Eolic Cell to Improve the Wind Velocity Augmentation Effect through the Metamodel of Optimal Prognosis.” *Energy Conversion and Management: X*, vol. 16, Dec. 2022, p. 100330, https://doi.org/10.1016/j.ecmx.2022.100330. Accessed 31 Mar. 2023.
[7] H. K. Versteeg and Weeratunge Malalasekera, *An introduction to computational fluid dynamics : the finite volume method*. Harlow: Pearson Education, 2007.

[8] I. Hashem and M. H. Mohamed, "Aerodynamic performance enhancements of H-rotor Darrieus wind turbine," *Energy*, vol. 142, pp. 531–545, Jan. 2018, doi: https://doi.org/10.1016/j.energy.2017.10.036

[9] A. Rezaeiha, I. Kalkman, and B. Blocken, "CFD simulation of a vertical axis wind turbine operating at a moderate tip speed ratio: Guidelines for minimum domain size and azimuthal increment," *Renewable Energy*, vol. 107, pp. 373–385, Jul. 2017, doi: https://doi.org/10.1016/j.renene.2017.02.006.

[10] Kemal Hanjalić, Y Nagano, and M. J. Tummers, Turbulence, heat and mass transfer 4 : proceedings of the fourth international symposium on turbulence, heat and mass transfer, Antalya, Turkey, 12-17 October, 2003. New York ; Wallingford: Begell House, 2003.

[11] "Procedure for Estimation and Reporting of Uncertainty Due to Discretization in CFD Applications," *Journal of Fluids Engineering*, vol. 130, no. 7, p. 078001, 2008, doi: https://doi.org/10.1115/1.2960953.

[12] T. W. Simpson, A. J. Booker, D. Ghosh, A. A. Giunta, P. N. Koch, and R.-J. . Yang, "Approximation methods in multidisciplinary analysis and optimization: a panel discussion," *Structural and Multidisciplinary Optimization*, vol. 27, no. 5, Jun. 2004, doi: https://doi.org/10.1007/s00158-004-0389-9.

[13] D. C. Montgomery and G. C. Runger, *Applied statistics and probability for engineers*. Hoboken, Nj Wiley, 2018.

[14] W. H. Press, *Numerical recipes in FORTRAN : the art of scientific computing*. Cambridge England ; New York, Ny, Usa: Cambridge University Press, 1992.

[15] P. F. S. Trentin, P. H. B. de B. Martinez, G. B. dos Santos, E. E. Gasparin, and L. O. Salviano, "Screening analysis and unconstrained optimization of a small-scale vertical axis wind turbine," *Energy*, vol. 240, p. 122782, Feb. 2022, doi: https://doi.org/10.1016/j.energy.2021.122782.